UCRL-JC-119377
PREPRINT

Coupled Light Transport-Heat Diffusion Model for Laser Dosimetry with Dynamic Optical Properties

Richard A. London, Michael E. Glinsky, George B. Zimmerman,
David C. Eder, and Steven L. Jacques*

This paper was prepared for submittal to the
SPIE's 1995 International Symposium on Lasers
and Applications/Biomedical Optics
Laser-Tissue Interaction VI,
San Jose, CA
February 4-10, 1995

March 1, 1995

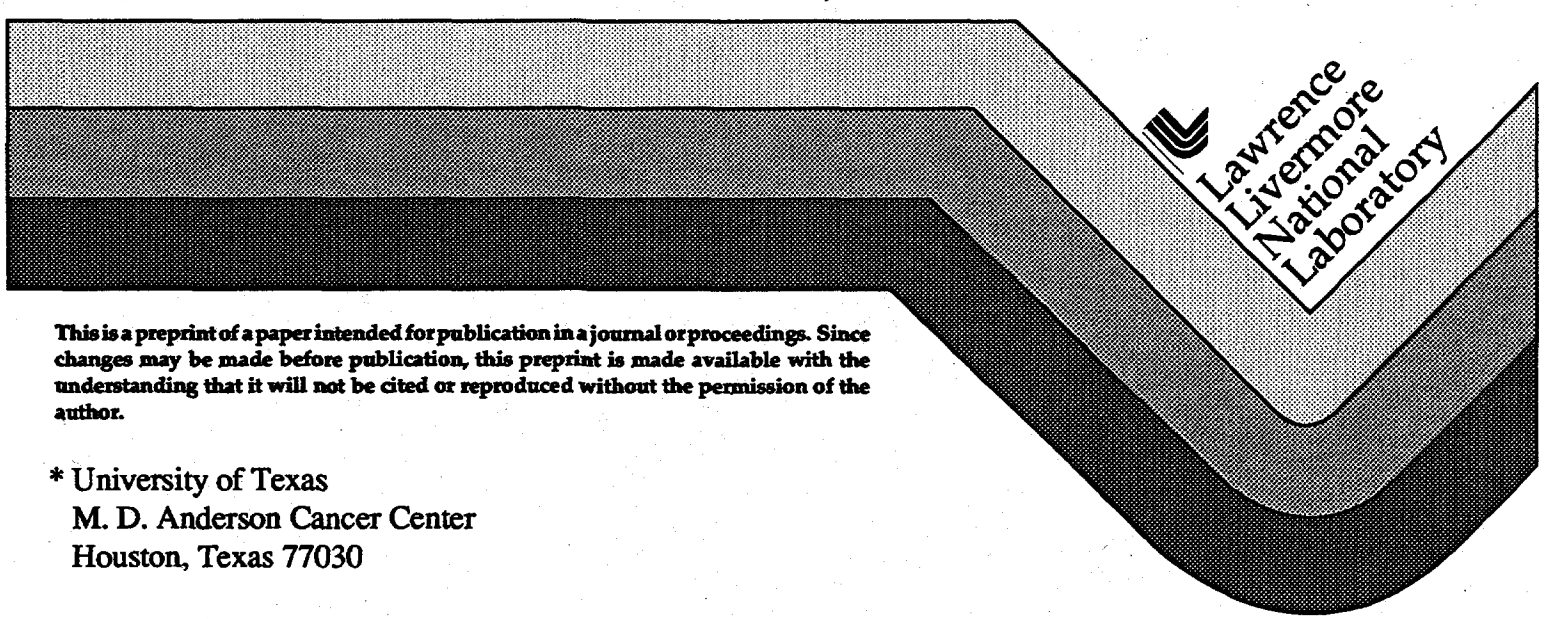

* University of Texas
M. D. Anderson Cancer Center
Houston, Texas 77030

Coupled light transport–heat diffusion model for laser dosimetry with dynamic optical properties

Richard A. London, Michael E. Glinsky, George B. Zimmerman and David C. Eder

Lawrence Livermore National Laboratory
Livermore, California 94550

and

Steven L. Jacques

University of Texas–M. D. Anderson Cancer Center
Houston, Texas 77030

ABSTRACT

The effect of dynamic optical properties on the spatial distribution of light in laser therapy is studied via numerical simulations. A two-dimensional, time dependent computer program called LATIS is used. Laser light transport is simulated with a Monte Carlo technique including anisotropic scattering and absorption. Thermal heat transport is calculated with a finite difference algorithm. Material properties are specified on a 2-D mesh and can be arbitrary functions of space and time. Arrhenius rate equations are solved for tissue damage caused by elevated temperatures. Optical properties are functions of tissue damage, as determined by previous measurements. Results are presented for the time variation of the the light distribution and damage within the tissue as the optical properties of the tissue are altered.

Keywords: dynamic optics, laser-tissue modeling, laser dosimetry, tissue damage

1. INTRODUCTION

Dynamic optics is defined as the alteration of tissue optical properties by laser irradiation. In this paper, we specifically consider changes in the scattering coefficient due to thermal damage in a photo-thermal therapy situation. In general, one is interested in how dynamic optics affect the total dose to the tissue, the size of the damaged region, and the reflected light pattern. We focus on the size of the damage region. We study how the dynamic optics effects vary with the laser irradiation and tissue parameters such as the laser spot size, the pulse length, the presence of cooling by blood perfusion, and the treatment of the scattering anisotropy. The paper is laid out as follows: section 2 discusses the physical elements of the model and the computer code, section 3 states the tissue properties used for this study and section 4 presents simulation results. Plans for future work and conclusions are presented in section 5.

2. FUNDAMENTALS OF THE NUMERICAL MODEL

A coupled laser light transport–heat diffusion numerical model is used. Time-dependent simulations are done on a two-dimensional spatial domain with cylindrical geometry. The model is embodied in a computer code called LATIS, which models laser-tissue interactions considering four areas of coupled physical processes, as illustrated in Figure 1.

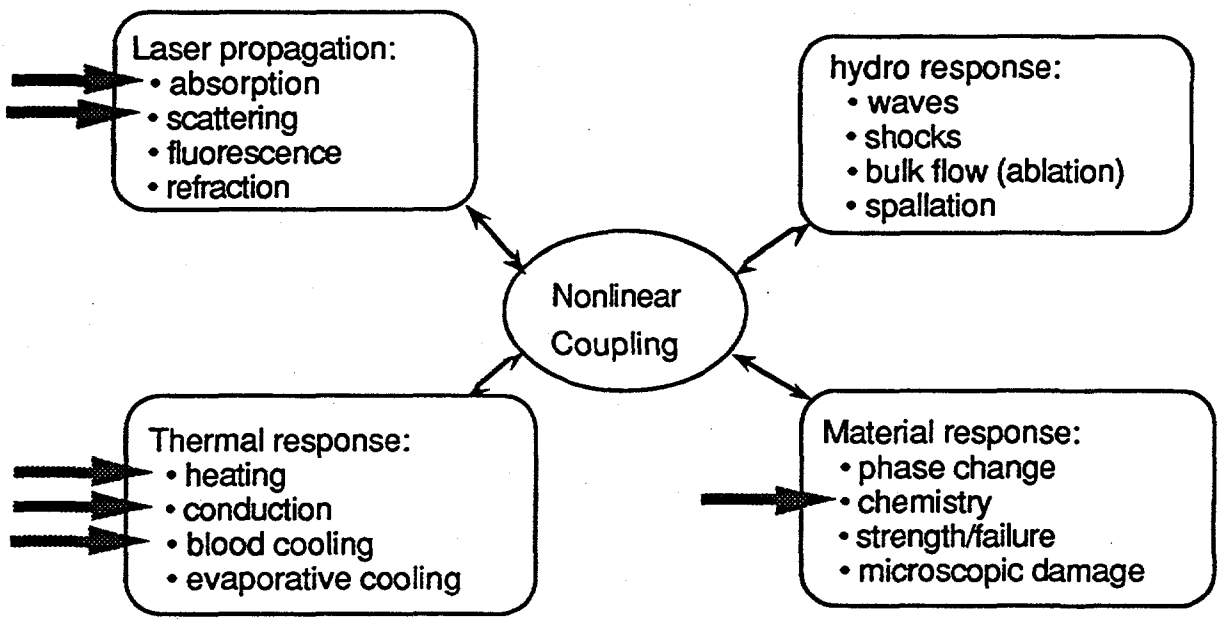

Figure 1. LATIS models laser-tissue interactions considering four areas of coupled physical processes. The arrows indicate features used for the present simulations. Features such as the hydro response are being developed for future use in tissue ablation applications.

LATIS is based on 20 years of experience in modeling laser-matter interaction for the Laser-Fusion Program at LLNL. The current work represents an extension to new applications areas at much lower laser irradiances.

Light transport is calculated with a Monte-Carlo method. Photons are followed time dependently, although the light travel timescales are all very short compared to other timescales in the current cases. A fixed number of photons is introduced into the problem for each time-step. For most of the calculations in this study 300 photons/time step were used. Results changed insignificantly when 1000 photons were used. Scattering is calculated with a Henyey-Greenstein phase function. Absorption is calculated analytically without destroying the photons. Each photon is assigned a weight which decreases with absorption. When a photon's weight drops below 1%, it is retired from the Monte-Carlo calculation. The absorbed energy is tabulated in spatial zones where it serves as a source which elevates the tissue temperature and drives the heat diffusion.

Heat diffusion is calculated by a finite difference solution of the diffusion equation on a spatial mesh. A blood perfusion cooling rate is included in the energy equation for the tissue. The net cooling is equal to a temperature and damage dependent coefficient times the temperature above body temperature. The temperature dependent coefficient increases linearly by a factor of 4 between 37 °C and 42 °C to model increased perfusion due to vessel dilation. It is constant at temperatures above 42 °C. The damage dependent coefficient is an exponential cutoff in the perfusion with the damage integral (see below) to account for vessel coagulation.

Damage to the tissue is calculated with an Arrhenius rate model. We use a damage integral:

$$\Omega = \int k\, dt, \text{ where the damage rate, } k = \frac{k_b T}{h} \exp\left[\frac{\Delta S}{R} - \frac{\Delta H}{RT}\right], \qquad (1)$$

where k_b and h are the Boltzmann and Planck constants, respectively, and ΔS and ΔH are the entropy and enthalpy of the reaction, respectively. The undamaged fraction of the tissue is $f_u = \exp(-\Omega)$ while the damaged fraction is $f_d = 1-f_u$. The dynamic scattering coefficient is a linear combination of an undamaged and a damaged coeffiicient: $\mu_s = \mu_{su} f_u + \mu_{sd} f_d$. The variation of μ_s with damage integral in illustrated in Figure 2.

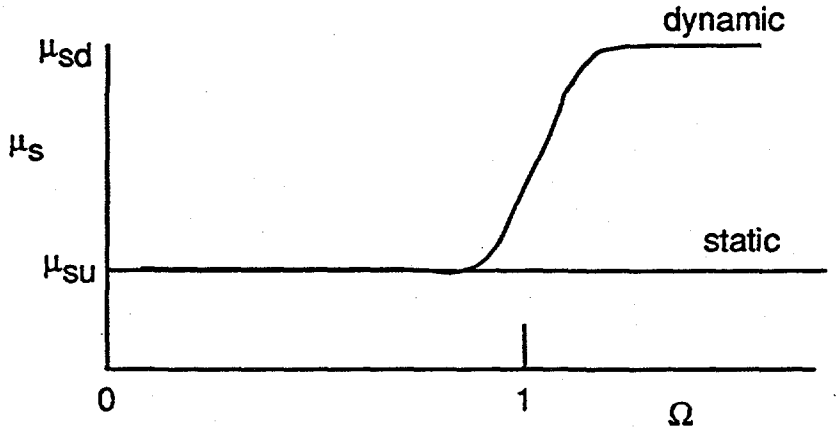

Figure 2. The scattering coefficient varies with damage integral. For static optics cases the scattering coefficient is kept fixed at the undamaged value.

3. TISSUE PROPERTIES AND STANDARD CASE

We choose characteristic, but "generic," tissue properties in order to demonstrate the capabilities of our modeling code and to illustrate the physical effects involving dynamic optics. The optical properties are those of dog myocardium at 630 nm. The scattering coefficients are $\mu_{su} = 50\ cm^{-1}$ and $\mu_{sd} = 350\ cm^{-1}$. The scattering anisotropy factor is g=0.9. The absorption coefficient is fixed at $\mu_a = 0.3\ cm^{-1}$. Such parameters are also tyical of many other soft tissues in the 630–800 nm range.

Damage rate coefficients are fit to average data for whitening of several sample tissues:

dog prostate, dog heart and rat and pig liver. The entropy used in Eq. (1) is $\Delta S = 68.2$ cal/mole and the enthalpy is $\Delta H = 45.79$ kcal/deg/mole. With these coefficients, the damage timescale (1/k) varies rapidly with temperature: from 100 s at 65 °C to 0.5 s at 90 °C. In the simulations the temperature is kept near 72.5 °C at which the damage timescale is 20 s.

Thermal properties (heat capacity and conductivity) are taken to be those of water. We do not consider phase changes such as the vaporization of water.

We define a standard case with the following parameters: laser pulse length= 60 s, laser spot size (radius) = 1 mm, scattering anisotropy factor = 0.9 and blood perfusion rate = 0.4 ml/g/min. We present results for the standard case and then consider variations of the parameters about these values in section 4.

The laser focus is assumed circular and the tissue is assumed initially homogeneous. The laser irradiation is taken to be flat-topped in space with a certain radius. We model a finite cylinder of tissue as indicated in Figure 3.

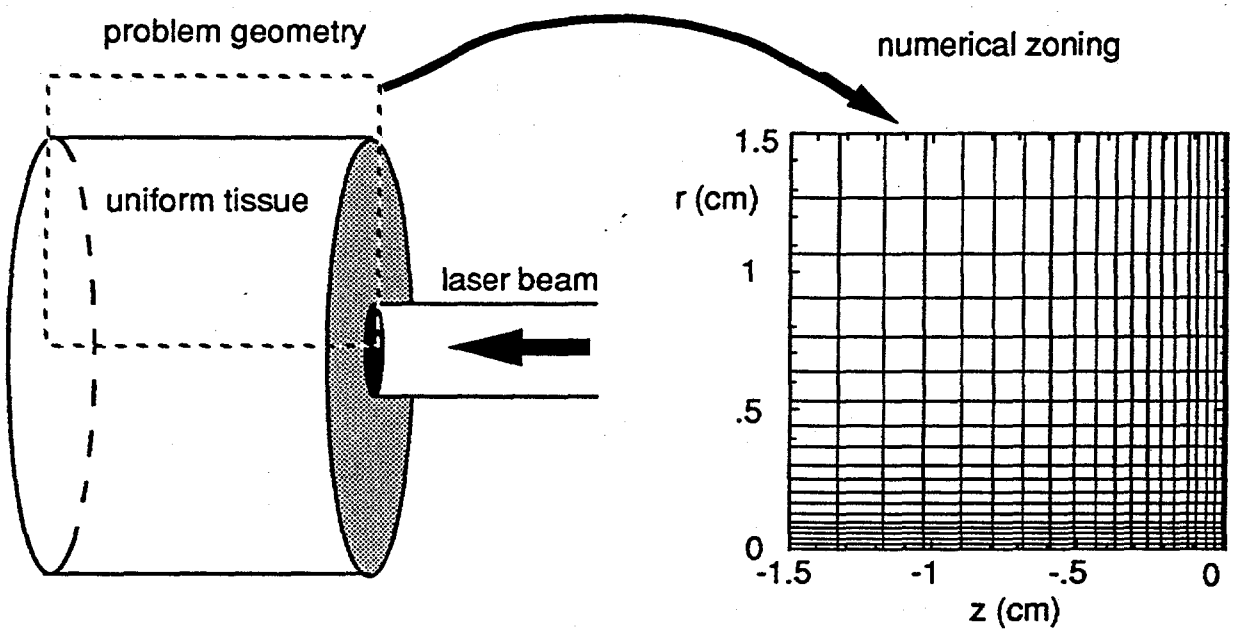

Figure 3. The laser-tissue irradiation is modeled in cylindrical geometry with fine zoning near the laser spot and course zones far from the spot.

The zoning is set up to have fine zones near the laser focal spot where the highest resolution is desired. The zone sizes grow outside the spot, reaching large values far from the laser deposition region. This zoning techniques increases the problem resolution while maintaining a relatively small number of zones.

The laser intensity is controlled by a thermostat function which keeps the surface temperature of the directly irradiated region within a desired range. We actively control the laser intensity by monitoring the average temperature in a 3x3 set of tissue zones within the laser spot. We turn the laser off when the temperature exceeds the desired maximum and

then turn it back on when the temperature drops below the desired minimum, as indicated in Figure 4. This technique enables a very good control of the damage progress and avoids adverse effects associated with dehydration and/or vaporization as temperatures approach 100 °C. Such a temperature control technique has recently been shown experimentally using infra-red radiometry by several groups[1,2].

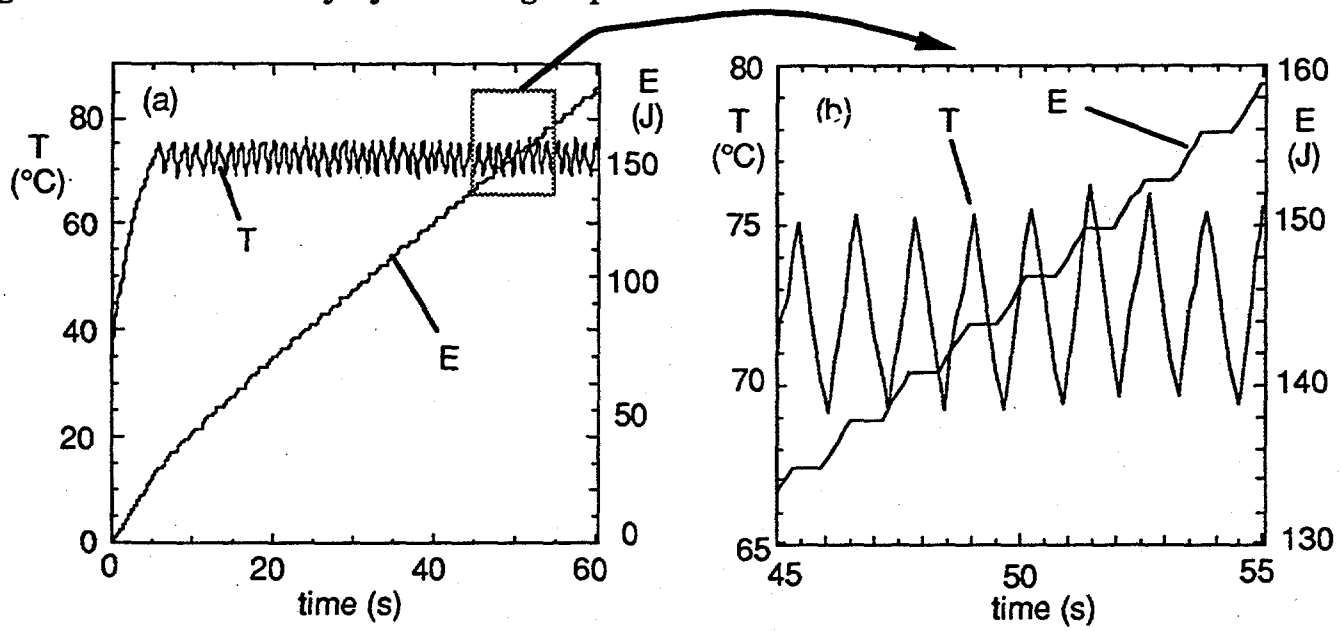

Figure 4. The surface temperature is kept within a desired range by a thermostat function. Here the range is between 70 and 75 °C. The time integrated laser energy shows the periods when the laser is off as flat sections.

4. SIMULATION RESULTS

Results for the distribution of absorbed laser energy and the damage zone for a simulation of the standard case are shown in Figures 5a and 5b. The absorbed laser light reflects the time-average light distribution, since the absorption coefficient is constant. The distribution shown in Figure 5a is for the end of the 60 s pulse, but similar patterns are apparent at earlier times. The temperature distribution (not shown here) extends further away from the laser focal region, owing to heat diffusion. The size of damage zone, as indicated by the Ω=1 contours of Figure 5b, grow in time, due to both the thermal diffusion beyond the energy deposition region and the increasing time for accumulation of damage.

We now turn to the effect of dynamic optics on the size of the damage zone. We compare the damage zone (Ω=1) for the standard case with dynamic optics to that with static optics in Figure 6b. By static optics we mean a simulation in which the scattering coefficient is kept fixed at its undamaged value, even though the tissue becomes damaged, as indicated in Figure 1. It is clear that the inclusion of dynamic optics reduces the size of the damage zone. To measure this reduction we define a damage ratio as the depth of the damage zone with dynamic optics relative to that without dynamic optics: D = z(Ω=1) dynamic/ z(Ω=1) static. For the standard case we find D=0.67. In Figure 6b, the case of a larger spot size

(r=0.5 cm) is shown. Here the effect of dynamic optics is somewhat less than for the standard case; the damage ratio is 0.77.

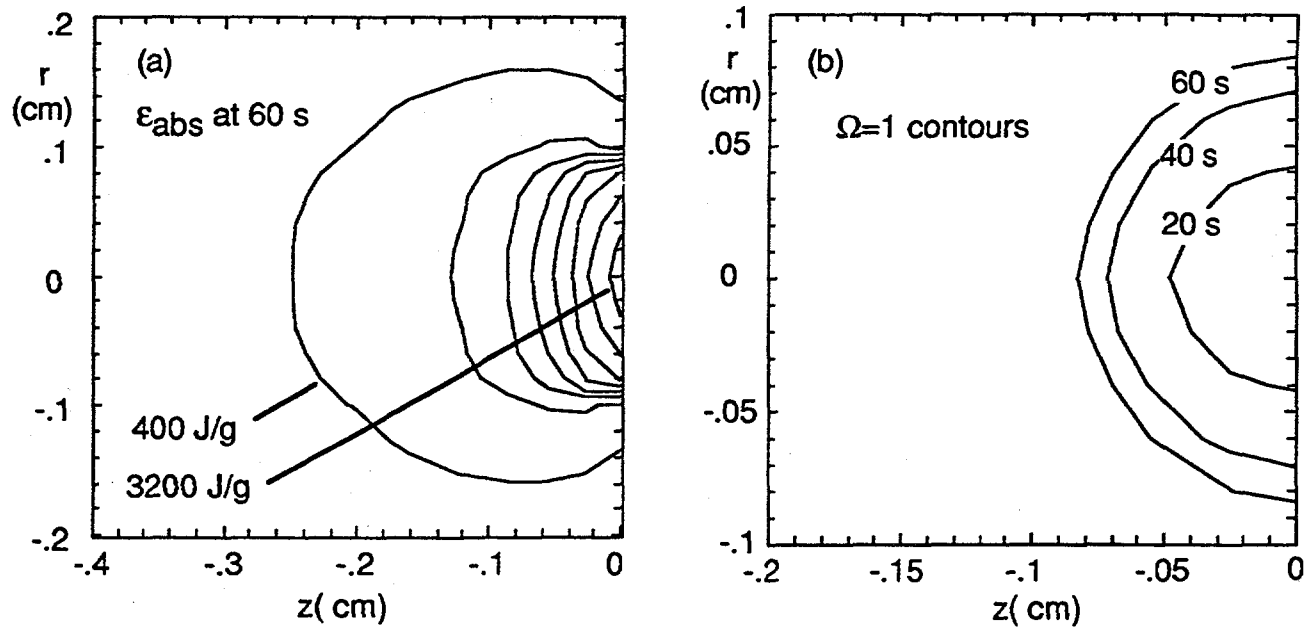

Figure 5. The total absorbed energy density integrated over the 60 s pulse is shown in Figure 5a. Laser and tissue conditions are for the standard case. This pattern reflects the light distribution. The damage region (Ω=1) is shown at various times during the pulse in 5b. It grows due to heat diffusion and time-accumulation of damage.

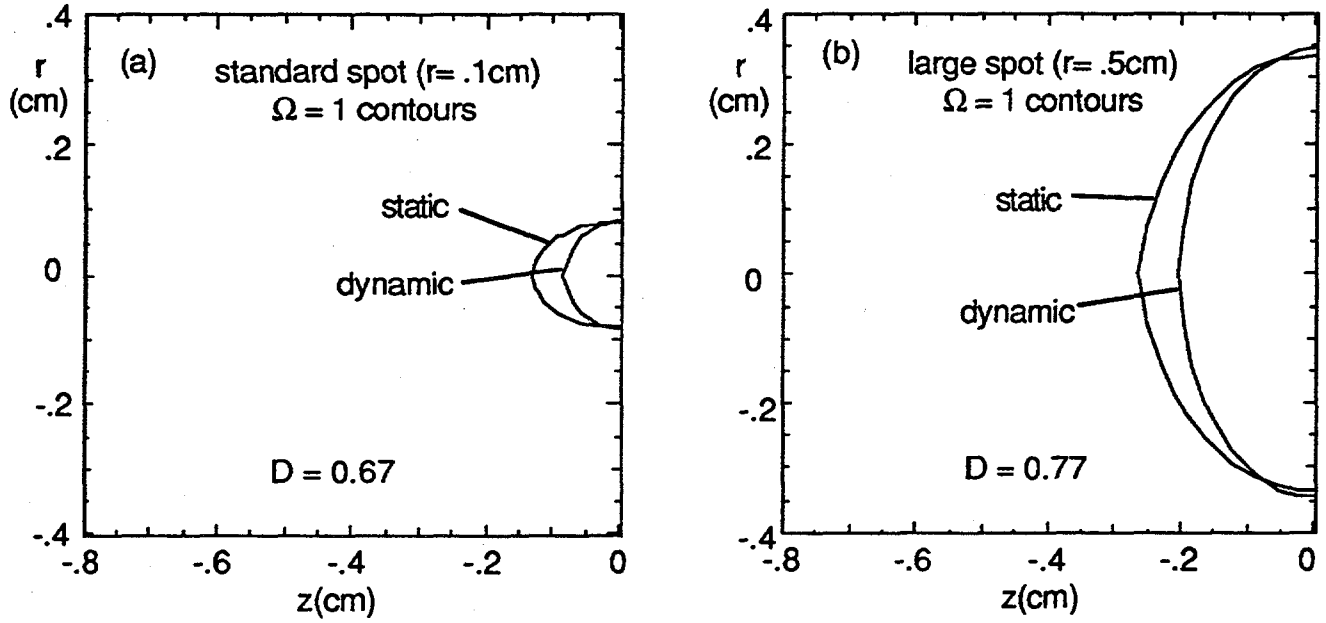

Figure 6. The size of the damage regions is reduced by dynamic optics, as shown for the standard case in Fig. 6a and for a case with a large spot in 6b. The effect of dynamic optics is greater for the standard spot than for the large spot. All curves are for the end of the pulse (at 60 s).

A study has been done to acertain the sensitivity of the reduction in the damage zone caused by dynamic optics to other parameters. For each parameter variation, we have performed 2 simulations–one with dynamic optical coefficients and one with static coefficients. We then form the damage ratio as the ratio of the depth of the Ω=1 contour with dynamic optics to that with static optics. The parameter variations and resultant damage ratios are listed in Table 1.

Table 1. Damage ratio versus parameter variations

variation	$D \equiv \frac{Z(\Omega=1)\ \text{dynamic}}{Z(\Omega=1)\ \text{static}}$
standard case:	0.67
short pulse (20 s)	0.76
long pulse (180 s)	0.63
small spot (0.01 cm)	0.39
large spot (0.5 cm)	0.77
isotropic scattering	0.67
no blood perfusion	0.66

We show results for the spot size variations and the pulse length variations graphically in Figure 7.

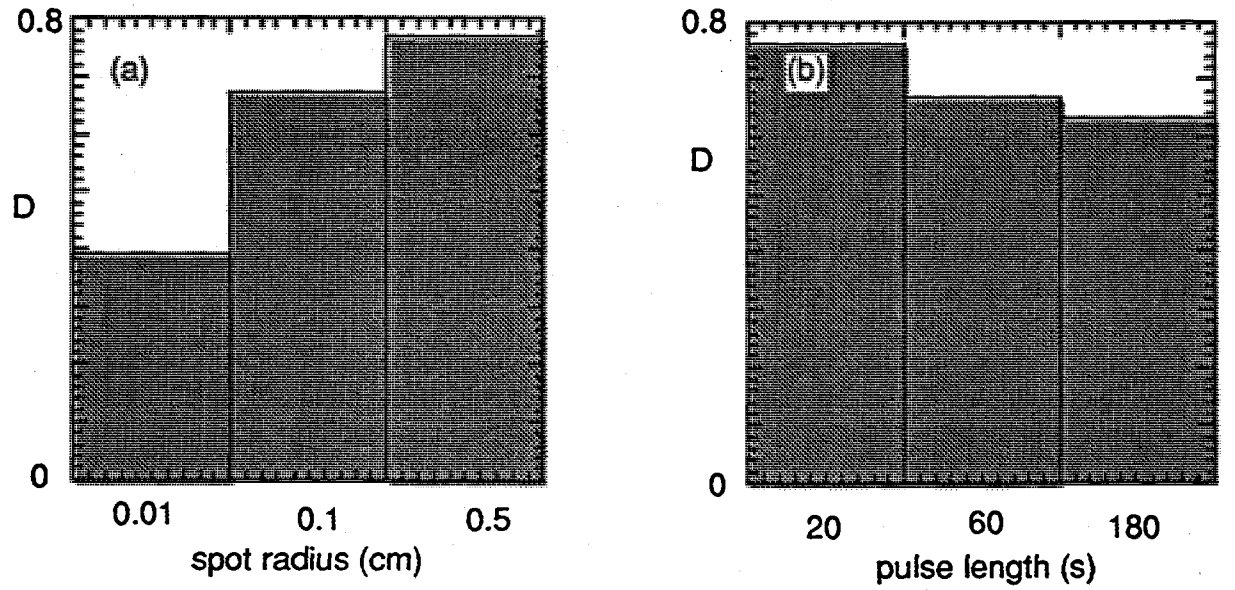

Figure 7. Variation of the damage ratio with spot radius (a) and pulse length (b). The variations can be understood by comparing the spot size to the laser penetration depth and the pulse length to the damage timescale at the surface temperature.

The variation with spot size can be understood by comparing it to the diffusive optical penetration depth $\delta = [3\mu_a(\mu_s + \mu_a)]^{-1/2}$. For the undamaged tissue δ= 0.46 cm while for the damaged tissue it is 0.18 cm. For spot sizes large compared to δ, (the case of 0.5 cm) the deposition region is properly given by δ which scales like $\mu_s^{-1/2}$. For small spot sizes the laser light scatters out of the beam, leading to smaller deposition region, scaling approximately as μ_s^{-1}. This higher dependence on μ_s leads to the relatively larger effect of dynamic optics for the smaller spots.

The variation with pulse length stems from the relationship to the typical damage timescale. We have controlled the surface temperature to an average value of 72.5 °C, which gives a characteristic damage timescale of 20 s. Thus short pulses of about 20 s or less will not have enough time to produce a large damage zone and will therefore show less difference between the dynamic optics and the static optics cases, as illustrated in Figure 7b.

Variations in the isotropy of scattering and the blood perfusion rate were also explored. The isotropic scattering case assumed smaller scattering coefficients, so that the "reduced scattering coefficient", $\mu_s' = \mu_s(1-g)$, was the same as for the standard case with g=0.9. This was found to have very little effect on the simulation results. The case with no blood perfusion showed 10% larger damage depth in both dynamic and static cases, but very little differential effect, as seen from Table 1.

In summary we see that dynamics optics reduces the depth of damage by about 33% in most cases. The laser spot size and pulse length effect the reduction factor as illustrated in Figure 7.

5. CONCLUSIONS

In this paper, we have described a numerical technique for the calculation of optical dosimetry problems with dynamic optics. A computer program–LATIS–which embodies this model has been presented. Simulations results for a simplified laser therapy situation have been presented. The effect of dynamic optics has been explored and correlated with variations in the laser and tissue parameters. We have found that dynamic optics can cause a significant reduction in the size of the damaged region. For most cases studied this reduction is about 33%. Laser spot size and pulse length are important parameters in determining the effect of dynamic optics.

Several areas have been identified for improvements to the model. The damage model should be improved to deal directly with measure rates and to consider multiple-rate processes. Improvements in the blood perfusion model should account for transport of heat to adjacent tissue regions. Evaporative and flow enhanced convective cooling from tissue surfaces should also be modeled in the future.

With enhancements to the model presented here, we intend direct comparisons to experimentally measure quantities such as interstitial temperature and light distribution and coagulation region size in order to validate and update the model. Our model has direct relevance to the design of specific clinical experiments and protocols such as prostate

coagulation for treatment of benign prostate hyperplasia, percutaneous fiber delivered coagulation of liver metastases and coagulation of gastro-intestinal tumors

We now have the ability to model complex laser dosimetry problems and will be addressing more realistic experimental and clinical problems in the future.

ACKNOWLEDGEMENTS

This work was performed under the auspices of the U. S. Department of Energy by the Lawrence Livermore National Laboratory under contract number W-7405-ENG-48.

REFERENCES

1. B. Lobel, O. Eyal, E. Belotserkovsky, O. Shenfeld, N. Kariv, B. Goldwasser and A. Katzir, "In-vivo CO_2-laser rat urinary bladder welding with silver halide fiberoptic radiometric temperature control," *in Laser Welding: Modeling, Delivery Systems, and Tissue Solders,* Eds. L. S. Bass, et al., Proc. SPIE 2395D (in press, 1995)

2. I. Cilesiz, E. K. Chan, S. L. Thomsen, and A. J. Welch, "Controlled temperature tissue fusion: cryogenic Ho:YAG laser welding of rat small intestine in vivo," *in Laser Welding: Modeling, Delivery Systems, and Tissue Solders,* Eds. L. S. Bass, et al., Proc. SPIE 2395D (in press, 1995)